ELIoT: enhancing LiFi for next-generation Internet of things

Please check the document version of this publication:

• A submitted manuscript is the version of the article upon submission and before peer-review. There can be important differences between the submitted version and the official published version of record. People interested in the research are advised to contact the author for the final version of the publication, or visit the DOI to the publisher's website.
• The final author version and the galley proof are versions of the publication after peer review.
• The final published version features the final layout of the paper including the volume, issue and page numbers.
Link to publication

ELIoT: enhancing LiFi for next-generation Internet of things

J. P. M. G. Linnartz[1,2], C. R. B. Corrêa[1*], T. E. B. Cunha[1], E. Tangdiongga[1], T. Koonen[1], X. Deng[1], M. Wendt[2], A. A. Abbo[2], P. J. Stobbelaar[2], P. Polak[2], M. Müller[3], D. Behnke[3], M. Martínez[4], S. Vicent[4], T. Metin[5], M. Emmelmann[5], S. M. Kouhini[6], K. L. Bober[6], C. Kottke[6] and V. Jungnickel[6]

*Correspondence:
c.ribeiro.barbio.correa@tue.nl

[1] TU Eindhoven,
5612AZ Eindhoven, The
Netherlands
[2] Signify, 5656AE Eindhoven, The
Netherlands
[3] Weidmüller Group,
32758 Detmold, Germany
[4] MaxLinear, 46980 Paterna,
Valencia, Spain
[5] Fraunhofer FOKUS, 10589 Berlin,
Germany
[6] Fraunhofer HHI, 10587 Berlin,
Germany

Abstract

Communication for the Internet of things (IoT) currently is predominantly narrowband and cannot always guarantee low latency and high reliability. Future IoT applications such as flexible manufacturing, augmented reality and self-driving vehicles rely on sophisticated real-time processing in the cloud to which mobile IoT devices are connected. High-capacity links that meet the requirements of the upcoming 6G systems cannot easily be provided by the current radio-based communication infrastructure. Light communication, which is also denoted as LiFi, offers huge amounts of spectrum, extra security and low-latency transmission free of interference even in dense reuse settings. We present the current state-of-the-art of LiFi systems and introduce new features needed for future IoT applications. We discuss results from a distributed multiple-input multiple-output topology with a fronthaul using plastic optical fibre. We evaluate seamless mobility between the light access points and also handovers to 5G, besides low-power transmission and integrated positioning. Future LiFi development, implementation and efforts towards standardization are addressed in the EU ELIoT project which is presented here.

Keywords: Future IoT, LiFi, Optical wireless communication, Light communication, IEEE 802.11bb, ITU-T G.vlc

1 Introduction

The amount of wireless data traffic and the number of devices continues to grow at an exponential rate. This puts high pressure on the radio spectrum. Over the past decades, we have seen waves of innovation to enhance the bit rates (bit/s) and the density (bit/s/m^2) that can be provided by wireless radio networks, but the wireless technology needed to support this also becomes increasingly complex. For instance, massive multiple-input and multiple-output (MIMO) and beam-steering in 5G push the radio technology frontiers but may run into limits of complexity and power consumption also for signal processing and for conversion between analogue and digital domains.

Reaching limits with RF motivates the industry into exploring new directions including optical wireless communications, which is also denoted as LiFi [1]. For light waves, walls, ceiling and floor are natural boundaries between the wireless cells that

Linnartz *et al. J Wireless Com Network*   (2022) 2022:89

Page 2 of 33

allow very dense reuse of a vast amount of optical spectrum. Light sources such as light emitting diodes (LEDs) can offer gigabits per second transmission with simple emitters and receivers, with the potential for a very low cost.

The concept of communication via light is older than via radio. However, when local area networking (LAN) went wireless in the 1990s, the demand for achieving coverage across multiple rooms was larger than the desire to very densely reuse the radio spectrum, as at that time, not many devices were using it. That favoured radio solutions. Meanwhile, since the 1990s, Wi-Fi and cellular technologies became ubiquitous. The majority of the increased capacity is due to steadily reduced cell sizes as the need to serve many more users in dense areas grew. Extrapolating these trends explains the increasing interest in LiFi, which can cover small "personal" cells with very high data rates. Moreover, such a dedicated beam experiences and causes little interference from other users, thus can guarantee undisturbed, low-latency traffic to its destined user.

Particularly, the Internet of things (IoT) can be seen as a driving force behind further densification. The IoT is often characterized by a vast multitude of many devices that each generate only limited traffic, but collectively cause a substantial increase in traffic. However, as Fig. 1 also illustrates, we foresee numerous future IoT applications that demand higher rates, lower latency, and increased link reliability. Examples are in factories with Industry 4.0 machines, industrial devices or smart glasses [2, 3]. In particular, we see an increasing need for low-latency, guaranteed bandwidth combined with positioning not only in augmented reality but also in real-time control of industrial processes. LiFi is a promising approach to address these future needs, possibly combining the wider through-the-wall coverage of RF networks with high-density very small cell high quality of service (QoS) LiFi, as seamless handovers and a common security approach appear to be feasible, as work in this paper demonstrates. For instance, RF communication may be well suited for many devices each with a modest bit rate, while in addition LiFi can fill in QoS demanding hotspots.

The first LiFi systems are now deployed commercially, and further innovation and new features are needed to exploit their full potential in an increasing number of use cases and applications. This paper highlights how these challenges are addressed in the EU H2020 project ELIoT (Enhance Lighting for the Internet of things). As this is an overview paper, extending our EuCNC paper [4] we refer the reader to multiple

Fig. 1 Some IoT use cases targeted by the ELIoT project

Linnartz *et al. J Wireless Com Network*   (2022) 2022:89

Page 3 of 33

publicly available project papers for more details. In particular, the main contributions reported are:

- Providing and testing interworking with other systems such as the radio and wired infrastructure, in particular with 3GPP and 5G.
- Providing a viable approach to integrating positioning within the communication standard
- Allowing mobility to other LiFi access points via MIMO link adaptation (horizontal mobility) and to other technologies, in particular with Wi-Fi and with 5G (vertical mobility) while protecting against outages from light beam blockage.
- Proposals for introducing MIMO and experimental performance verification by related G.hn home networking standards.
- Developing cost-effective and easy-to-install in-building backbone infrastructure networks, for instance, plastic optical fibre (POF).
- Demonstrating end-to-end security concepts and comparing 5G and IEEE 802.1 × approaches to security.

2 Method

This paper addresses results achieved in the ELIoT research to create technical improvements to make LiFi more mature, in particular via MIMO, multicasting, LiFi-5G integration, POF front-hauls, and positioning technology, which are to be contributed to standardization. We followed the method of initially identifying use cases and their specific demands for improvements. Secondly, on initial visible light communication (VLC) test networks at our partners' we landscaped the state-of-the-art using available advanced prototypes. In this way, the shortcomings of current solutions have been identified and based on this input, ELIoT conceived, developed, implemented and tested identified potentially innovative ceiling architectures, components, protocols and algorithms, which were validated independently and in parallel by multiple partners. Results from building experimental set-ups were captured in new models and translated into transferable building blocks. Yet, this also required us to develop an overarching reference architectural view. These have been reviewed in the following stage for consistency and compatibility with standardized protocols and algorithms.

This paper follows an outline that starts with this architectural view in Section III. Specific results on security and mobility support can be seen as more or less independent protocol functionalities and are presented and discussed in Sections IV and V, respectively. Further architectural results are presented and discussed in Section VI for the cell layout, Section VII for the fronthaul, and Section VIII for the MIMO PHY. The step to ensure valorization via standardization is discussed in Section IX. A further enhancement by adding positioning, beyond the primary communication functionality is described in Section X.

3 LiFi concept

There are many interesting applications for LiFi in different environments, such as office, industrial, in-home or outdoor [5]. Each of these poses different requirements, so a rigid single-use system concept may not be appropriate. However, cost and scalability

considerations dictate that solutions for the various use cases can be served flexibly by functional components, exploiting commonalities and reusability of hardware and software. In fact, network integration of LiFi as a layer 2 LAN, equivalent to a classical Ethernet connection, is needed and provides good versatility by supporting various protocols such as the internet protocol (IP) or industrial automation protocols, see Fig. 2. A common physical layer (PHY) and medium access (MAC) convergence format are important for harmonization. It addresses the key commonality of use cases and solutions.

The most widely used LiFi PHY makes use of direct current (DC)-biased orthogonal frequency division multiplexing (OFDM) with adaptive bit loading to allow scalability and exploit the full capacity of LiFi. Distributed MIMO (D-MIMO) is an attractive extension as it supports spatial multiplexing and diversity [6, 7]. In fact, for industrial-grade QoS, MIMO appears key to avoiding link outages if a line of sight (LoS) is blocked [8].

As further elaborated in Section VI.B, D-MIMO using spatially separated optical front ends (OFEs) can avoid frequent handovers associated with the small optical cell size, thus ensuring consistent QoS and reliability for high mobility and high user densities. The MIMO PHY preferably is based on subcarrier-wise channel estimation. It can be based on the feedback of the channel state information (CSI) but can also exploit generic low-pass properties of LEDs [9]. To support battery-constrained devices, a low-power PHY can be very useful. Pulse amplitude modulation (PAM) at a low rate, e.g. below 3 MHz bandwidth, proved to be effective in the uplink or in a VLC downlink. OFDM signals in higher parts of the modulation spectrum, e.g. beyond 5 MHz, can coexist with such PAM signals.

To ensure QoS with guaranteed throughput and latency, the channel access mechanism is reservation-based, using spatial time-division multiple access (spatial TDMA), similar to Space–Time Reservation Multiple Access [10]. Power saving through scheduled sleep periods yields longer battery lifetimes.
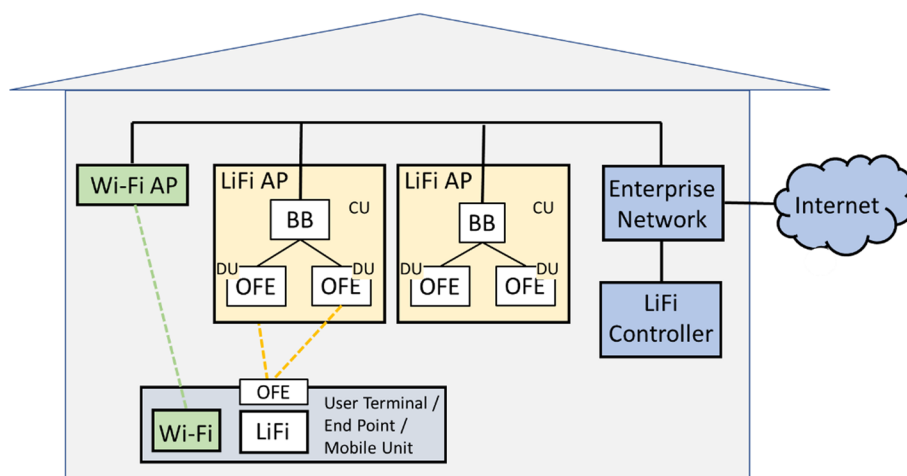

Fig. 2 Indoor system architecture overview comprising LiFi and Wi-Fi: each LiFi access point (AP) has a LiFi central unit (CU) that performs the baseband (BB) PHY and MAC layers and connects to multiple distributed units (DUs) which are optical front ends (OFEs) in the ceiling. The user terminal is also referred to as mobile unit (MU)

The backhaul connects the LiFi infrastructure to a fixed access network with a common interface to the higher layer services. This backhaul network may be realized over different media, such as Ethernet, power line communications (PLC) and POF, each having its own capacity and latency characteristics. Whether or not a separate power infrastructure is needed for active OFEs can also be a key design consideration if the cost of the backbone is critical. A transparent ("analogue, jitter free") fronthaul network allows versatile integration and upgradability. The identified main functional components of LiFi connectivity can be combined in order to build practical solutions for different use cases. Extended functionality for specific solutions can be realized through software modules in the CU (only). Further advanced functions can be link monitoring to facilitate vertical handovers, remote configuration based on standard protocols, as well as QoS management and service metering.

Extending Fig. 2, a LiFi system concept for an industrial scenario has been investigated in ELIoT [3, 11], and the concept may also be used in other situations. The concept is based on large-scale distributed MIMO to cope with the line-of-sight characteristics of light and the required QoS. A key aspect of our approach is to scale up the number of OFEs that are controlled by a single AP to cover larger areas. This AP can execute the PHY and MAC processing in a synchronous manner for all OFEs. As a result, moving users stay connected as the AP dynamically selects the appropriate set of OFEs. This enables virtually seamless connectivity without the need for handover protocol procedures. Moreover, centralized signal processing for the distributed OFEs facilitates the use of synchronous MIMO schemes to increase link robustness and throughput further. Figure 3 applies this to an industrial context.

Depending on the context, such APs are in the literature and in standardization referred to as central units (CUs) and distributed ceiling nodes, possibly luminaires, that are equipped with OFEs are denoted as distributed units (DUs), see Fig. 3. Each DU can reach terminals or end points like moving users in a certain area with its light cone. The cones of neighbouring DUs can overlap to provide homogenous coverage with adequate spatial diversity opportunities. There are multiple ways to split functionality between the CU and DUs [12, 13], but for indoor LiFi, we see an attractive approach in creating the waveforms in the CU and feed these over a transparent linear channel without digitization. A transparent and synchronous fronthaul network connects all DUs with their common CU. In fact, DUs are understood as the optical antennas of the CU, which
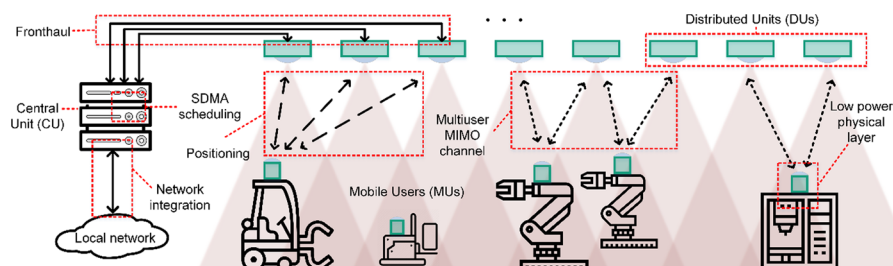

Fig. 3 Distributed multi-user MIMO system architecture, depicting a CU connected with DUs via a fronthaul network. Mobile and stationary devices communicate via the LiFi infrastructure at the same time. Several key aspects are indicated

receive analogue waveforms ready for transmission to and from the MUs. In the CU, the PHY defines the transmitted waveform, including error coding and modulation, and aids the MAC through measuring the channel. As we will elaborate in Section V, because the CU controls all MIMO processing for its DUs and MUs in the whole coverage area, no exchange of PHY-layer information between multiple APs (CUs) is necessary. Mobility is adaptively supported by adapting the signals to DUs for each MU based on the channel state. This can be done in various ways, such as by approaches that are similar to antenna combining or selection in radio systems, or power loading based on a total power constraint or per-DU power constraint [14]. IEEE 802.15.13 already makes use of different PHYs for downlink and uplink transmissions which may be attractive for other standards, for instance in ITU G.9991, also known as G.vlc [15]. Both are chosen such that they support the different requirements for downlink and uplink in an optimal way. Because MUs may be battery-powered, the uplink PHY should be more energy-efficient and able to operate at a low signal-to-noise ratio (SNR) [16].

To select and track the best DUs based on the MU's mobility, an IEEE 802.15.13 scheduler in the CU considers the latest channel state. Moreover, the modulation and coding scheme (MCS) is selected carefully to optimize the rate while frame losses and increased latencies through retransmission are avoided. To obtain the necessary information for this scheduling, the CU assesses the channel between all its DUs and the MUs periodically. Moreover, features such as multi-user access and conflict-free scheduling are supported [11, 17].

Accurate positioning is considered an enabling feature for wireless communication in factories, e.g. to locate automated guided vehicles. For integrated positioning, the high-speed OFDM PHY can perform sub-sample accurate timing measurements based on a conventional ranging (also denoted as timing advance) aided by additional phase estimation in the frequency domain. If this approach is combined with distributed MIMO, the MAC can triangulate the position of the terminal and reach centimetre precision [18]. A detailed description of our approach can be found in Section X.

4 Indoor positioning

Besides communication, smart manufacturing calls for positioning to facilitate various new Industry 4.0 applications. For example, reliable indoor positioning is necessary for using intelligent transport systems (ITS) that transport parts on pallets from predefined locations to other predefined locations. It is usual that transport systems in factories and warehouses travel along predefined paths, defined by inductive loops or optical markers on the floor. But these systems are not flexible, and modifications need effort. LiFi enables localization beyond predefined paths and allows extended positioning use cases due to more degrees of freedom. For example, a transport system can determine a new path on-demand to drive around an obstacle that occurred on the planned path. In addition, there are new opportunities when production resources can be located on-demand. For example, its position can be displayed on a digital factory map. This makes it possible to find a tool, a container with raw material or (semi-) finished products needed in a few seconds, which supports the work of machine operators and production planners. In addition, real-time positioning of mobile devices can support technical maintenance staff or production managers. For example, tablets can support them by using

the position information to display position-based information such as dashboards with machine data of the nearest machine(s).

In the ELIoT project, we propose to realize positioning based on a multi-lateration algorithm, which measures the wireless propagation times between a mobile device and multiple LiFi APs at the ceiling [19, 20]. The ranging or timing advance algorithms for positioning are well understood and used in fixed and mobile access systems [18]. The accuracy of the result depends primarily on the quality of estimating the time-of-flight. To address the inherent synchronization challenges between mobile and ceiling units, an active ping-pong protocol is used to measure the round-trip time. This allows, in combination with standard techniques for clock offset estimation, an accurate estimation of the time-of-flight. The overall principle of LiFi-based positioning is shown in Fig. 4 [18]. Figure 4a shows the ranging by multiple transmitter units, Fig. 4b the signal structure based on the G.hn standard and Fig. 4c the ping-pong protocol for the estimation of the round-trip time. To confirm this concept, a series of simulations and measurements have been carried out in ELIoT. First results [18] showed the feasibility of the concept through simulations in a 3D environment as well as by ranging experiments of LiFi point-to-point links. Further investigation addressing 3D positioning scenario is presented in this section. The set-up is shown in Fig. 5 and consists of 4 Tx units at fixed positions and a single Rx unit. The signal progressing, as shown in Fig. 4, is performed in MATLAB and the signal conversion by DACs and ADCs. For the measurements, the Rx units were at multiple positions and the performance at each of them was evaluated.

Figure 6 shows the estimated (blue circle) versus the actual positions of the receiver for 40 measurements (iterations) at each of the 12 positions. The transmitter positions are indicated by the triangles. The difference between estimated and real receiver positions is overall very small, with a higher deviation towards the edges of the room. Figure 7a shows the resulting average mean-square errors (MSE), for each the *x*-,*y*- and *z*-axis and for each Rx location taking 40 independent measurements into account. The x-axis shows generally higher MSEs and the errors of the z-axis are the smallest, with one exception. The smaller error for the z-axis can be attributed to the alignment of
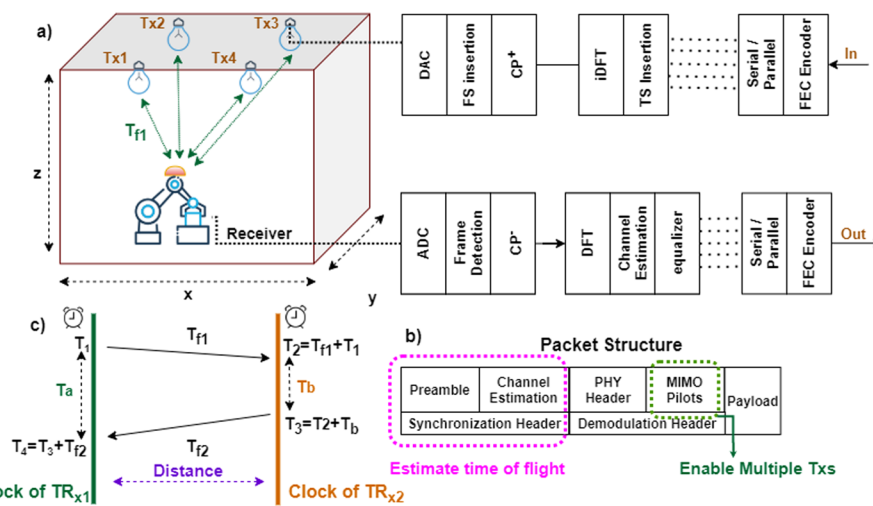

Fig. 4 **a** + **c** Principle of LiFi-based positioning, **b** signal structure

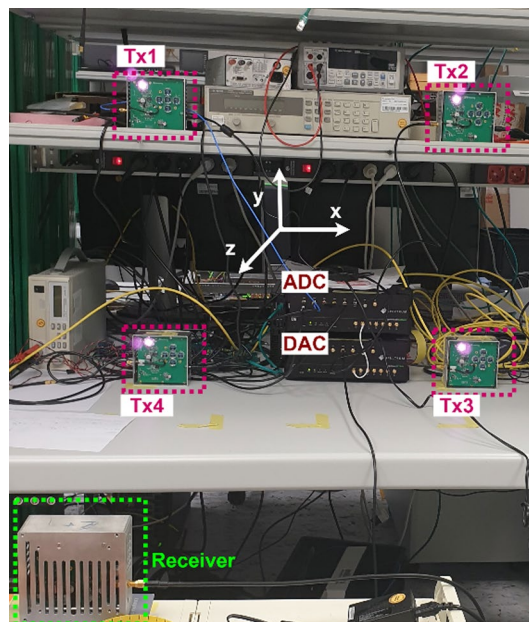Linnartz *et al. J Wireless Com Network*   (2022) 2022:89

Page 8 of 33

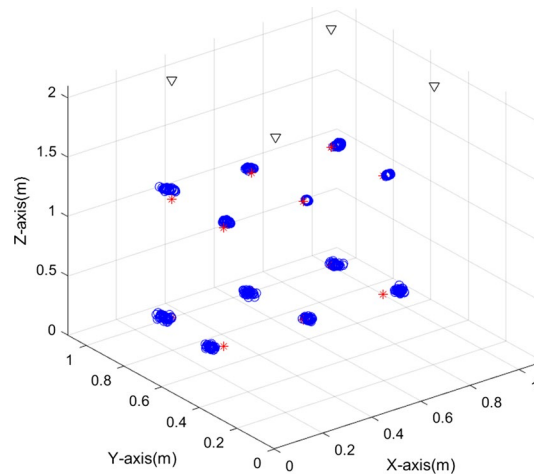**Fig. 5** Measurement set-up for 3D evaluation

Fig. 6 Estimated (denoted by blue circles) versus real position (denoted by red stars) for multiple receiver positions. Transmitter positions are denoted by triangles

the set-up. In Fig. 7b, the combined x, y, z error is shown for three Rx positions over 40 measurements. There are two observations: First, there is a different offset error for each position, with Rx(1,0.72,0) the highest and Rx(0.67,0.725,0) the lowest. The offset error can be attributed to non-ideal calibration, which was only performed in 1D for one location only. Note that the offset error is smaller in the centre position between the four transmitters (blue curve) and is higher at the edges (red curve). Second, there is a second type of error caused by the signal noise. This random error is indicated by the variation around the offset error, and its magnitude is directly related to the SNR and to the distance between Tx and Rx. The offset error can be minimized by a more careful initial calibration of the system before the actual measurements and the second error
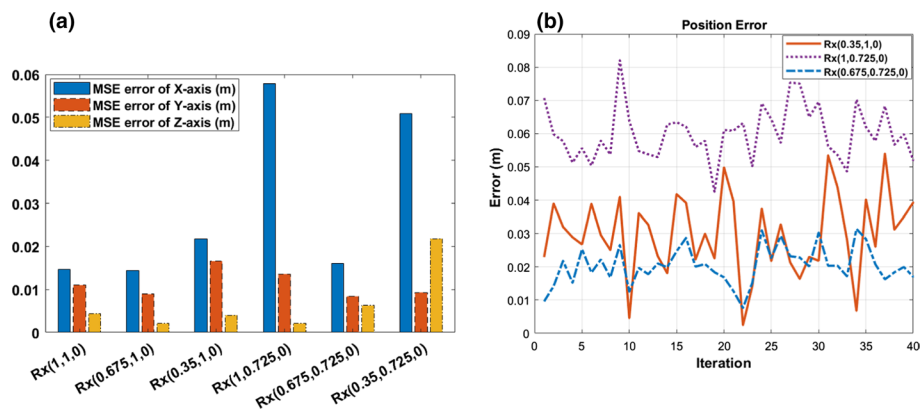
Linnartz *et al. J Wireless Com Network*   (2022) 2022:89

Page 9 of 33

Fig. 7 Mean square error (MSE) of *x, y, z* for selected Rx position (**a**) and combined error or three receiver positions over 40 measurements (**b**)

by applying a stronger averaging, i.e. taking more measurements for each position into account.

4.1 Possible roadmap for adding positioning to G.vlc

Enabling real-time positioning requires integration into a LiFi chipset. Today's chipsets only partly support the proposed concept. The ELIoT project is working with a chipset from MaxLinear that implements the ITU-T G.9991 recommendation [21]. With this chipset, a coarse round-trip time estimation can already be achieved by using the time tagging capabilities. More precise timing information can be extracted from the channel frequency response (CFR) as demonstrated by the ELIoT experiments. For a next-generation chipset, new APIs have to be developed in the PHY to provide information on the SNR and CFR to the higher layers.

The high-level architecture of the digital baseband G.9991 chipset is shown in [21] (page 9). The baseband chip decodes the frames coming from the channel and injects frames into the channel through an analogue front-end chip that performs the signal adaptation to the medium. The positioning techniques explained here and in [18] would run on application programming interfaces (API) and can already be partially implemented using commercially available chipsets. The chipset can make use of some of the functionalities and framing of the standard that allow refining the procedure explained in [21].

5 Security (results and discussion)

LiFi is said to be inherently more secure than radio. Light can be easily kept inside a room and signal levels outside a main light beam are inadequate to eavesdrop on the signal. The inherent protection against a jamming attack on a large industrial installation or factory hall becomes increasingly important in Industry 4.0 settings with autonomous devices. Nonetheless, this view disregards many types of potential attacks. So, we rather phrase the property that light stays inside the room as adding an additional layer of security. However, this does not obviate the need for proper encryption, authentication, access control, key management and hardware device security. If LiFi is used in security-critical settings, the "digital" security needs to be

at least as good as is common practice for radio-based infrastructures. For instance, bringing a hacked LiFi device into a secured area should not compromise the complete LiFi network security. IT departments or operators prefer to rely on security mechanisms that are compatible with commonly used industry standards, such as Wi-Fi-compatible or 5G-based approaches, respectively.

The operator-focussed approach taken in ELIoT sees LiFi as a new access technology for non3GPP access to 5G network systems. The secured connection for the non-3GPP access to 5G is accomplished through the encapsulation and encryption of the transferred packets. A 3GPP technical specification [22] has introduced a new component called the Non-3GPP Interworking Function (N3IWF) which is responsible for the access and session operations between the user equipment (UE) and the core network (CN). It realizes IPSec tunnelling from the UE to the N3IWF to control the data security in both 5G control and user planes. Internet key exchange (IKE) and extensible authentication protocols authorization and key agreement (EAP-AKA) generate the key pairs for packet encryption and decryption. In this way, encapsulation and protection of LiFi communications comply with common security standards.

A second approach, which is appropriate for enterprise networks, provides compatibility with the IEEE 802.1X standard [23]. This approach makes any LiFi device operates in a similar way to a Wi-Fi device. The IEEE 802.1X standard defines a port-based network access control and authentication protocol that prevents an unauthorized client device from connecting to a LAN through publicly accessible ports unless they are properly authenticated. As shown in Fig. 8, IEEE 802.1X systems use a standard client/server architecture including the following three components:

• A **Supplicant,** which is a software module running on the terminal device to be authenticated and providing credentials to the authenticator using EAPOL frames [23]. The credentials are provisioned in advance by the network administrator, and could include a user name/password, shared key or a cryptographic certificate [24].

• An **Authenticator,** which is a software module running on the access point that controls the access of the terminal device to the network, and that relays the communications between the authenticating device (using EAPOL frames towards the AP) and the authentication server (using RADIUS protocol towards the AP) [25].
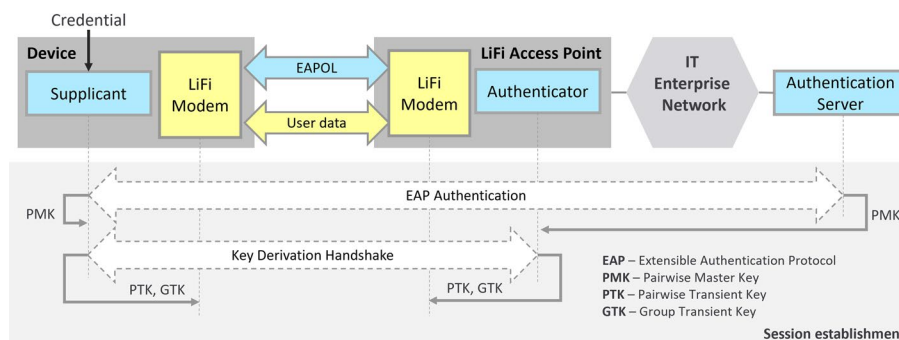

Fig. 8 LiFi enterprise network deployment using IEEE 802.1 × including the Supplicant, Authenticator and Authentication Server

•An **Authentication Server,** which maintains the trust relationships between terminal devices and the access network that can receive and respond to requests for network access originating from a terminal device running the supplicant. The server can evaluate the access requests and inform the authenticator if the connection is to be allowed for the device requesting access. The authentication server runs software supporting the RADIUS and EAP authentication protocols [26].

The authentication exchange is carried out between the supplicant and the authentication server with the authenticator acting as a relay for the EAP messages, see Fig. 8. The EAP messages carrying the EAP method-specific data are transported using EAPOL frames between the supplicant and the authenticator and RADIUS protocol between the authenticator and the authentication server, as shown in Fig. 9.

The authenticator facilitating EAP between the supplicant and the authentication server ensures that no user data can be transferred through the access point before the device is granted access and the secure session establishment involving device authentication and key derivation is finalized.

The following steps are performed for the secure session establishment:

- **Device and network authentication** through EAP method handshake between the supplicant and authentication server using pre-provisioned credentials, which results in both, the supplicant and the authentication server, in a common master key: pairwise master key (PMK).
- **Transfer of the PMK from the authentication server to the access point**
- **Key derivation handshake** like a 4-way handshake for Wi-Fi defined by [27] performed between the terminal device and the access point by using the master key, resulting in a set of specific transient keys: pairwise transient key (PTK) and group transient key (GTK) keys.

The PTK and GTK keys resulting from the key derivation handshake are used to derive session keys used to secure the data exchanged between the LiFi endpoint node in the client device and the LiFi access point over LiFi link. Once the session keys are derived, the device is granted access to the network and a secure channel is established between the client device and the access point allowing user data to be securely exchanged. This concludes the session establishment exchange.
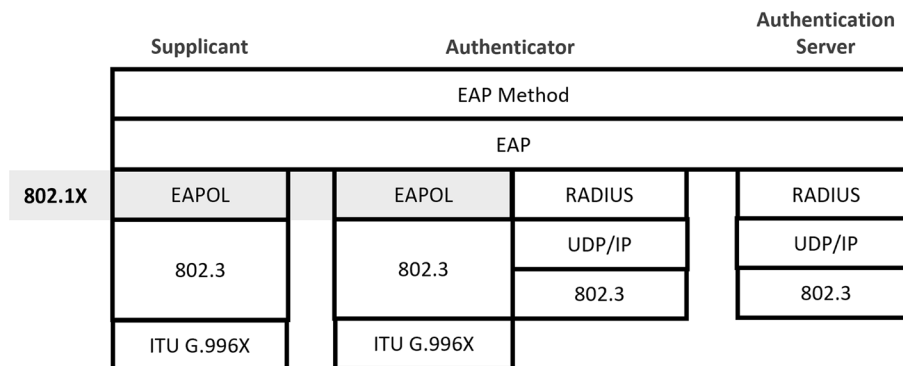

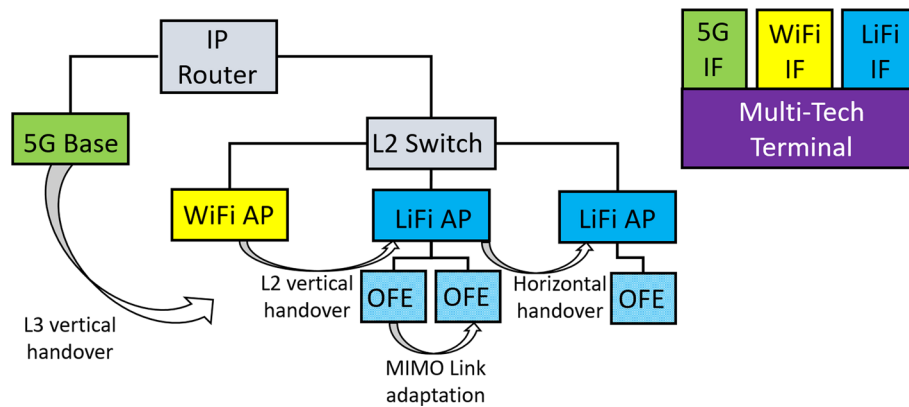**Fig. 9** IEEE 802.1 × port-based network access control protocol stack

Linnartz *et al. J Wireless Com Network* (2022) 2022:89

Page 12 of 33

Fig. 10 Handover scenarios between LiFi, Wi-Fi and 5G

Table 1 Handover definitions between LiFi, Wi-Fi and 5G

Term	Description/definition
MIMO link adaptation	A single AP optimizes the use of multiple OFEs to aid end point mobility. Association remains in the AP
Horizontal handover between non-overlapping and overlapping areas	Transfers of association state between two APs of overlapping LiFi cells. This is independent of the interference coordination between the APs
L2 vertical handover	Moves layer 2 connectivity between a Wi-Fi network and a LiFi network. The terminal's MAC address is preserved
L3 vertical handover	Moves IP-level connectivity of a terminal between different access technologies. The terminal's IP address might be preserved. Integration into 5G core network

This approach provides not only full control over who is joining the enterprise network but also the flexibility of supporting anyone of the standardized EAP authentication methods within the same infrastructure. A standardized set of commonly used protocols ensures that LiFi connectivity can easily be incorporated into any enterprise IT infrastructure.

6 Mobility support (results and discussion)

Seamless large-area coverage involving multiple LiFi APs and the integration of radio-based networks like 5G and Wi-Fi are important topics in ELIoT. Different handover scenarios are investigated, each with different characteristics and requirements. Moreover, security and access aspects are addressed to allow the integration of LiFi into existing Wi-Fi and 5G radio networks [13]. Figure 10 shows the handovers studied, with the definition in Table 1 and a detailed description of various mobility scenarios below.

6.1 MIMO link adaptation within one LiFi AP

In this scenario, multiple OFEs provide LiFi access in a service area (e.g. a single room) via a common AP that adapts its MIMO PHY layer if mobility demands so. Through other OFEs, the LiFi AP keeps the connection to the terminal alive even if the line of sight towards one OFE is accidentally blocked. Moreover, if the terminal is moved or rotated, the connection is maintained. The LiFi AP and terminal may optimize link

Linnartz *et al. J Wireless Com Network*   (2022) 2022:89

Page 13 of 33

performance by taking advantage of the light traveling via different signal paths. This is realized by using the D-MIMO technology. If a terminal moves within the coverage area of the LiFi AP, the latter can adapt the connection to the terminal by changing the selection of an active subset of OFEs for this terminal and by adapting the physical layer parameters (e.g. bit loading) for optimal link quality. The LiFi AP can trade off between robustness and power consumption. For robustness, the AP may activate all its OFEs for a terminal. To reduce power consumption, the AP may activate only the best OFE.

6.2 Horizontal handover: moving between APs with non-overlapping coverage areas

In this scenario, multiple areas are each served by a LiFi AP, whereby these areas are optically separated. This is typically the case for the situation of multiple (small) rooms in a building. No interference occurs between APs. If a terminal moves from one area to another, it typically enters an intermediate area (e.g. a corridor) without LiFi coverage and loses LiFi connectivity temporarily. As soon as the terminal re-enters an area with LiFi coverage, it re-connects (rapidly) to LiFi.

6.3 Horizontal handover: moving between APs with overlapping coverage areas

In this scenario, a large area such as an open office space is served by multiple LiFi APs, each covering part of the total area. Now the coverage of APs intentionally overlaps to prevent dead zones. A terminal in an overlap area connects to one AP, while the interference has to be managed, e.g. by coordinating APs. The motion of terminals across service areas is similar to Wi-Fi: a terminal can initiate a handover. This could be a "break before make" handover, whereby the LiFi link is lost, but most preferably a "make before break" handover is supported to keep breaks of the LiFi link short.

LiFi will have much smaller cells than Wi-Fi and more abrupt cell fringes. This demands a fast handover. A terminal therefore preferably anticipates a handover by pre-registering to a neighbouring AP and pre-establishing security keys via the currently active connection and the backhaul. The line-of-sight propagation characteristics of LiFi require adequate handling of interference and hidden-terminal problems. A terminal typically sees the APs, but not any of the other terminals. An AP sees terminals but not the neighbouring APs. Hence, carrier-sense multiple access (CSMA) may not prevent APs (or terminals) from transmitting at the same time. LiFi preferably uses coordinated medium access. This also strengthens the ability to guarantee QoS, by organizing the medium access so that the link is not hampered by interference.

6.4 L2 vertical handover: moving in/out of LiFi area within a Wi-Fi area

In this scenario, a small area is served by LiFi (e.g. a single room), while a larger area is covered via Wi-Fi (e.g. in a hallway or in less intensively used rooms). For a terminal that moves in or out of the LiFi area, a vertical L2 handover between LiFi and Wi-Fi takes place. A terminal in the LiFi area can offload the traffic from Wi-Fi and increases its QoS. A terminal that moves out of the LiFi area keeps a connection through Wi-Fi, as shown in Fig. 10. Ideally, by aggregating two wireless techniques, their throughput is added. In the IEEE 802.11 standard, L2 handover is defined by fast basic service set (BSS) transition and fast session transfer. As LiFi is not yet tightly integrated into 802.11, alternatively, integration of both techniques can be realized via the IEEE. 1905.1 standard. In

fact, 1905.1 existed already for some time but gained popularity as the Wi-Fi mesh technology reuses clauses from it.

6.5 L3 vertical handover in 5G context

Integration of LiFi into radio-based 5G connections requires an L3 vertical handover [13]. This enables a user to freely move between both 3GPP-trusted and untrusted access systems. The implementation in ELIoT of such a handover is shown in Fig. 11.

Building blocks on the left-hand side of Fig. 11 consist of a user terminal, e.g. a PC, which has parallel connections to the application server, by LiFi and by 5G new radio. The application server runs the 5G Core Network using software-defined networking (SDN). The radio connection, i.e. the air interface, takes place on the 3GPP radio access network (RAN). As a mediator, gNodeB is used, which represents the 5G RAN, and the core network, which is responsible to investigate the access operation. A second connection is created over an Ethernet interface ETH to the LiFi OFE, then through the actual LiFi wireless link to the infrastructure LiFi OFE, and finally via Ethernet to N3IWF coping with the integration of non-3GPP access technologies into the 5G packet core. In principle, the LiFi link is untrusted connectivity. Thus, the integration of LiFi into a 5G system mandates to encapsulate and encrypt packets between the user terminal and the N3IWF before these are transferred over the air; regardless of any link encryption. This operation for non3GPP access has been implemented in ELIoT. The responsible 5G network function is named N3IWF and it makes sure that the IPSec tunnelling is established without flaws to match the security standards [13]. In the case of link failures, the integrated system is capable of switching between these two access networks with very low latency and keeping user entities preserved.

7 Inter and intra-cell interference

To avoid that interference degrades performance inside cells or in overlap zones, one can divide the channel resources over the contending nodes. Multiple access is possible by time division (TDMA), modulation frequency division (FDMA), code division (CDMA) or wavelength division (WDMA), provided that a flexible MAC protocol can handle spatially conflicting demands. Radio systems, particularly those designed for unlicensed bands as used for IEEE 802.11, use carrier-sense multiple access—collision avoidance (CSMA/CA), that is, a node "listens before it talks". CSMA can flexibly handle random arrivals but may not guarantee QoS for ongoing sessions as it lacks the ability to reserve resources.
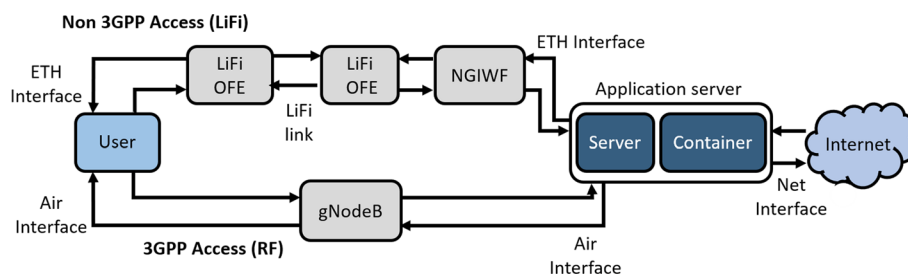

Fig. 11 LiFi-5G integration, as experimentally implemented at test set-up in ELIoT

As indoor LiFi networks use line-of-sight propagation characteristics, CSMA faces hidden node problems. An upward-looking MU or end point (EP) typically sees the downwards-faced OFE of the APs, but not any of the other EPs. An AP sees terminals but not the neighbouring APs. Hence, CSMA may not prevent APs (or terminals) from transmitting at the same time. LiFi preferably uses coordinated medium access within each cell. This also strengthens the ability to guarantee QoS, by organizing the medium access so that the link is not hampered by interference. In ELIoT, we focus on the ITU G.9991 standard that adopts TDMA for high QoS.

Continuous coverage implies that cells will overlap and potentially interfere with each other. So while moving between APs with overlapping coverage areas, not only a handover but also interference coordination of conflicting transmissions needs to be addressed spatially. A distinction from RF is that LiFi communicates via a directional LoS. This keeps the interference mostly localized to the overlap zone of the directly adjacent illuminated areas. This makes it possible to densely reuse the optical spectrum, so that the full high data rates become available at every machine location in a factory hall. In most cases, leakage into remote cells is negligible, which contrasts with rich multipath propagation in indoor radio systems. Our reference system contains ceiling-mounted LiFi APs while LiFi end points (EP) are spread in the area. Figure 12a depicts the coverage areas of AP1 and AP2 in solid grey and those of the EP1 and EP2 in dashed lines, respectively. EP1 is in an overlap zone for AP1 and AP2, both in up and downlink. Figure 12a shows how AP1 interferes with AP2 transmitting to EP2I. AP2 may not detect transmissions from AP1. Figure 12a also shows that EP2 is a hidden node for EP1. Although LoS propagation limits the coverage to a specific cell with only a small spillover, hidden node problems require mitigation as APs see EPs, but not other APs, while EPs see Aps, but not other EPs. So, in fact, a connection (in red) between AP2 and EP1 would be within coverage, but sees interference from hidden terminals in both directions.

LiFi is often promoted for its ability to provide contention-free QoS for ongoing sessions. In fact, TDMA allows coordinated scheduling. The network of APs determines the scheduling of the medium. Competition for access is resolved by coordinating the time schedules within and among adjacent APs, where the latter becomes a spatial extension of TDMA. A common channel (CC) may be established in order to facilitate the exchange of information between domains and facilitate detection of the interference.
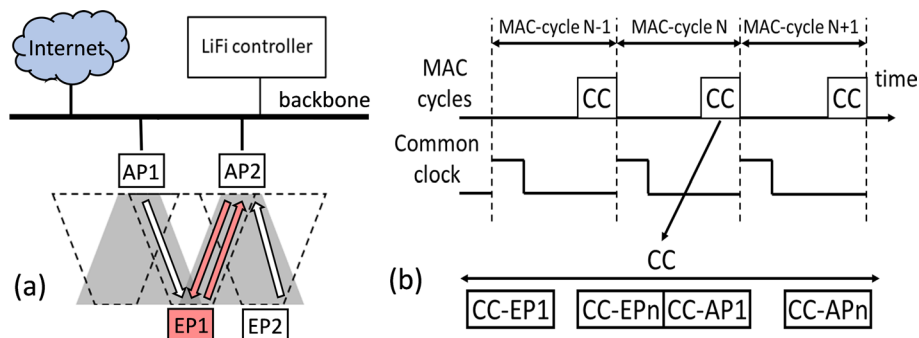

Fig. 12 LiFi network consisting of fixed APs and mobile user terminals EPs (**a**) and MAC cycle alignment to common clock and CC (**b**)

7.1 Spatial TDMA

The ITU-T G.9991 TDMA protocol can run as a specific firmware on ICs available for ITU-T G.9960/G.9961 [21]. ITU-T G.vlc separates the network into "domains". A LiFi domain can contain multiple cells, thus multiple CAs, and is seen as a part of a larger LiFi network. The domain concept may also fit to IEEE. 802.11 standard, if a LiFi domain is regarded as a BSS. All APs of one domain use a synchronized clock to ensure that TDMA frames are aligned across cells. Whether or not two neighbouring APs can simultaneously use the same time slot depends on the interference levels seen by EPs in the overlap zone [17]. In fact, the idea of dynamically assigning time slots not only in a time domain (TDMA) but also in spatial domain was launched in [28] and allows a virtual (cell-free) concept [29].

For optical wireless communications (OWC), ELIoT exploited the opportunity of connecting every domain via their AP to a backbone which exchanges inter-domain management messages via unique connections. Figure 12b shows this architecture. A dedicated LiFi controller (LC) handles and manages inter-domain contention, but does not act as a traffic router in the backbone. The LC observes instances of inter-domain interference and coordinates APs by setting constraints to their access schedules to avoid possible collisions, for instance using insights from [17]. The LC can be implemented as a central entity, but its functionality may also be distributed among the APs while the APs can nonetheless converge to a common, mutually coordinated scheduling. A common clock is shared among the domains to coordinate the MAC cycles in multiple domains. Figure 12b shows how APs are synchronized. This can be realized by running the precision time protocol (PTP) according to IEEE 1588 over the backbone. APs and EP terminals advertise their presence over a CC to detect potential inter-domain interference. Every AP tracks the activity of neighbouring nodes and reports interference events (collisions) to the LC, to allow it to set scheduling constraints for adjacent APs to resolve any conflicts. We illustrate this for the scenario in Fig. 12. In domain 1, EP1 receives advertisements of AP2 belonging to domain 2. AP1 flags this as an interference risk to the LC. In response, the LC constraints AP1 by only allowing the transmission to EP1 in a limited set of timeslots. It also constrains AP2 by prohibiting this set of slots in any communication with its own EPs. The algorithm to set time-division constraints is left as an opportunity for proprietary innovation, as it does not need to be fixed in ITU-T G.9991. A certification authority may be needed to ensure the interoperability of LCs, APs, and EPs from different vendors.

7.2 Handover-friendly and interference-mitigating cell layout

In a basic spatially extended LiFi network, every light point (e.g. a ceiling-mounted luminaire) can become an OFE or even a full AP, so cell boundaries and handovers can occur in the middle between two such light points. In RF-based WLAN systems, co-located antennas can offer MIMO gains because of the multipath nature of indoor radio propagation. For a rich scattering RF environment, an antenna separation of just half a wavelength is known to be adequate for creating independent, thus MIMO-separable streams. In LiFi, this mechanism of random multipath wave cancellation is not seen, because the detector itself spans thousands of wavelengths. Hence, even for

non-LoS LiFi with a rich scattering of intensity-modulated LC, the detector averages out multipath randomness by non-coherently adding photon flows. To achieve MIMO gains OFE separation needs to be much larger than the wavelength of the light; it needs to be larger than c/f, where f is the modulation frequency (10 to 100 MHz), thus many metres rather than micrometres. Co-location of optical MIMO OFEs in one device does not lead to independent channels, so a distributed architecture of MIMO OFEs is needed. Secondly, in optical propagation, the LoS is typically much stronger than the collective set of reflections, such that multipath does not yield a MIMO gain. Thirdly, and possibly most importantly, the LiFi channel statistics are dominated by blockage effects rather than by multipath wave cancellation.

If we consider these factors and the observation that the signal is most vulnerable in the middle between two light points where propagation distances are larger and where slant angles of arrival are more prone to blockage, we come to a cell layout, in which every cell is illuminated from its corners, as in Fig. 13. Inside the area, mobility is supported by MIMO link adaptation. Handover to an adjacent cell occurs right underneath each light point rather than halfway between APs. For the typical 60×60 cm ceiling tiles in offices, this calls for 90-degree corner sectors pointing into the cell with cell sizes of an integer multiple of the ceiling grid size, e.g. 1.8 or 2.4 m. The EP can of course rely on angular diversity and thus can be miniaturized.

The cell overlap zone now falls underneath an OFE and may be abrupt, thus the size of the overlap area will be mainly determined by the transition distance needed to execute a horizontal handover for typical EP speeds. For collimated sectors, thus when the sector boundary is sharply confined in azimuth rather than a gradually increasing lateral path loss, this handover line can be defined much more accurately for sector handover within one OFE, than for a transition somewhere halfway between two spatially separated OFEs. Reducing the overlap area also reduces the need for interference protection at the MAC layer, thus reducing the need for inhibiting potentially conflicting emissions, and thus the user capacity increases.
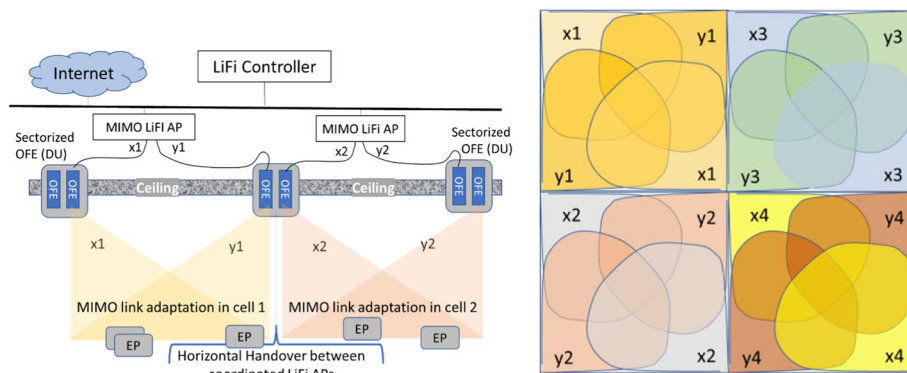

Fig. 13 LiFi cell layout that places cell boundaries along collimated sectors. Horizontal handovers take place on a well-defined line, while soft MIMO link adaptation takes place in areas in between APs. Left: cross section. Right: top view of MIMO channels x,y in cell 1, 2,…4

8 Broadband PHY fronthaul

As argued before, LiFi needs D-MIMO to protect against link blockage. This section presents a fronthaul infrastructure and identifies how the architecture of the fronthaul can be (cost-) optimized by leveraging the MIMO capabilities to jointly address wireless cross talk and possible cross talk in the fronthaul infrastructure. To explain that, we initially model the concatenation of a fronthaul and a wireless channel from a MIMO perspective.

The end-to-end channel, including wireless and fronthaul, from N_T emitters to N_R receivers is described by a $N_R \times N_T$ MIMO matrix $\boldsymbol{H}(f) = \boldsymbol{Z}(f)\boldsymbol{G}(f)$. That is the product of the cross talk coefficients from the POF fronthaul link represented by $\boldsymbol{G}(f)$ and the coefficients of the spatial overlap in the wireless channel given by $\boldsymbol{Z}(f)$. That is, we found that the $\boldsymbol{Z}(f) = \boldsymbol{Z}_0$ is mostly constant over frequency and that the response of $\boldsymbol{G}(f)$ mainly stems from known component properties. In fact, because of practical considerations only the ceiling OFEs, i.e. the DUs, can be spatially distributed, while at the client EP, angular separation of OFE co-located in the same miniaturized MU devices is preferred. $\boldsymbol{Z}_0$ originates from distance-related path losses, emission patterns and collimated receiver opening angles, while multipath reflections are weak. Thus, $\boldsymbol{Z}_0$ is independent of the modulation frequency. This structure in the channel matrix allows efficient implementation and limits protocol overhead. In fact, while we saw that in radio communication over mobile multipath channels, adaptive subcarrier-dependent loading requires prohibitive amounts of signalling overhead, in OWC over LEDs, it is very feasible, and actually proven within the ITU G.9991 to be effective and efficient.

To evaluate the throughput of a DC-biased optical OFDM (DCO-OFDM) D-MIMO link, a singular value decomposition (SVD) of the overall channel matrix $\boldsymbol{H}(f)$ is computed and the overall throughput is estimated by (1):

$$R = \Delta_B \sum_{n=1}^{N_{SC}} \sum_{k=1}^{K} \log_2 \left(1 + \frac{\text{SNR}}{N_T \eta_H \Gamma} \boldsymbol{\xi}_k^2(f_n) \right) \tag{1}$$

where Δ_B is the bandwidth occupied by each subcarrier, N_{SC} the number of subcarriers, K the rank of $\boldsymbol{H}(f)$, η_H the frequency–average path loss, $\Gamma = 10$ reflects typical system properties and, peak-to-average ratio (PAPR) DC biasing penalty [9, 19] and $\boldsymbol{\xi}_k(f_n)$ is the kth singular value of $\boldsymbol{H}(f)$ at the nth subcarrier. *SNR* is the signal-to-noise ratio referenced to the transmitter, thus defined as the transmit power P_T divided over the receiver noise spectral density N_0 times the total bandwidth $\Delta_B(f_N - f_1)$. The SNR can be influenced by spreading the power of the streams all over the frequency band in the most effective way within the power budget, but we assumed uniform power loading as done in ITU G.9991.

A simplified form is to use a single spatial stream with only one non-directional receiver photodiode (force $K=1$), but to emit this from multiple ceiling locations. Then, the signal strength becomes the sum of multiple beams, with some phase delay effects if the path length differs. In ELIoT, we evaluated and tested $K>1$ in various ways. In the next sections, we initially address the combined challenge of how to build a D-MIMO system and a corresponding ceiling infrastructure and subsequently test to what extent the existing solution (in particular [21]) can already address this or need to be improved.

8.1 Results on SDM and WDM-over-POF

POF can be attractive for the fronthaul of LiFi systems due to its do-it-yourself (DIY) ease of installation and its immunity against electromagnetic interference (EMI) [9]. To accommodate D-MIMO in the wireless link, two techniques can be used for POF-based LiFi fronthaul: space-division multiplexing (SDM) and wavelength-division multiplexing (WDM). SDM realizes point-to-point connections at the same wavelength over POF to connect each AP to the LiFi modem, as depicted in Fig. 14a. The main advantage of SDM is that there is no optical cross talk in the optical feeding network. For the WDM approach, a single feeder POF is used to distribute the signals to the various APs by using different wavelengths, as illustrated in Fig. 14b. WDM can simplify the installation and maintenance; however, it has higher complexity. With WDM, the amount of cross talk between channels can be significant, if there is overlap in the optical spectrum. The cross talk can be avoided using narrow optical light sources, such as laser diodes (LDs); however, a lower-cost system can be realized by using LEDs, which have a wider spectrum, thus higher spectral overlap. Yet, a new insight in ELIoT is that moderate colour cross talk in the POF is not necessarily harmful as it can be mitigated by end-to-end MIMO (matrix inversion) processing that will be applied for the wireless link [9, 30].

We measured SDM-over-POF with D-MIMO considering the channel response for the concatenation of POF and a wireless link. We only had access to commercially available red LEDs that would fit a POF connection, so we characterized the WDM-over-POF using LDs at 520 nm (green) and one at 658 nm (red). The WDM-over-POF
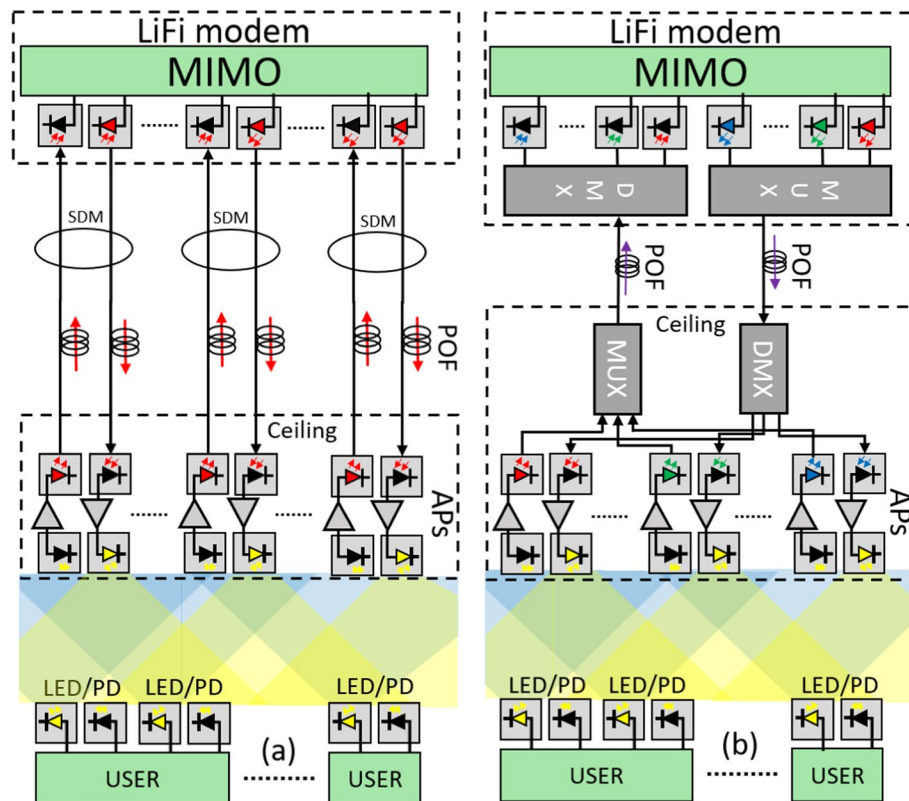

Fig. 14 **a** SDM and **b** WDM approach using POF as the fronthaul of LiFi

link is characterized by measuring the losses due to light absorption in the POF and the cross talk in the wavelength domain. We define cross talk as the leakage between adjacent channels that can occur due to insufficient channel separation in the demultiplexer (DeMux). Our DeMux has a cross talk level of -13 dB and 3.2 dB loss for the green channel and for the red channel a cross talk level of -25.7 dB and 3.6 dB loss [31]. The losses for the green and red channels are asymmetrical due to differences in emitting and received optical power and due to different receiver sensitivities for either wavelength. Considering only the optical link for WDM, a throughput of 2.5 Gbps is achieved for the green wavelength channel and 4.3 Gbps for the red wavelength channel. To evaluate the performance of WDM-over-POF with D-MIMO, the POF link and the wireless link channel response are measured separately and then combined. The experimental set-up is presented in Fig. 15, where d1 is the distance between APS and user receiver, d2 is the distance between receivers and d3 is the distance between the APs. Two measurement scenarios are implemented to represent the downlink of a high bandwidth multi-user MIMO transmission for LiFi. In the first scenario, the access points and users are located at $d_1 = 100$ cm, $d_2 = 70$ cm and $d_3 = 70$ cm. In the second scenario, the receivers are placed closer together, namely at $d_1 = 50$ cm, $d_2 = 5$ cm and $d_3 = 35$ cm.

From the singular values of $\boldsymbol{H}(f)$, seen in Fig. 16 with size 2×2, and considering an SNR of 20 dB, the achievable throughput of the system is calculated using (1). Table 2 reveals that the performance for SDM is, as expected, better than for WDM, but only slightly so. In SDM, the absence of spectral overlap leads to a better-conditioned matrix which increases the bit rate. Our WDM system further lacked margins to overcome unequal link budgets, which worsens after cross talk removal due to noise enhancement in the MIMO equalizer. In particular, with available components, the green channel appeared challenging due to lower optical power and lower responsivity at the receiver. In both scenarios, the red channel can carry more data. We observed that the optical WDM link in isolation provides high performance, but end-to-end throughput reduces when the wireless channel is concatenated. The SDM has been done with LEDs rather than with lasers. Nonetheless, the end-to-end link is mostly limited by the wireless channel rather than by the POF [9].
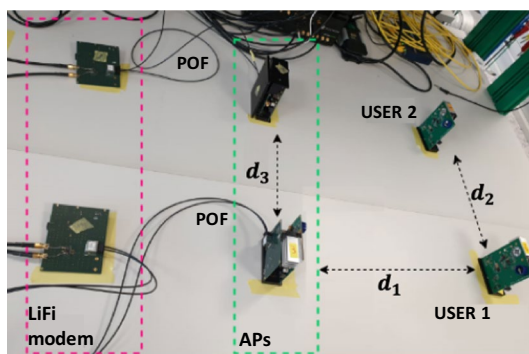

Fig. 15 Experimental set-up for LiFi D-MIMO using POF with SDM approach
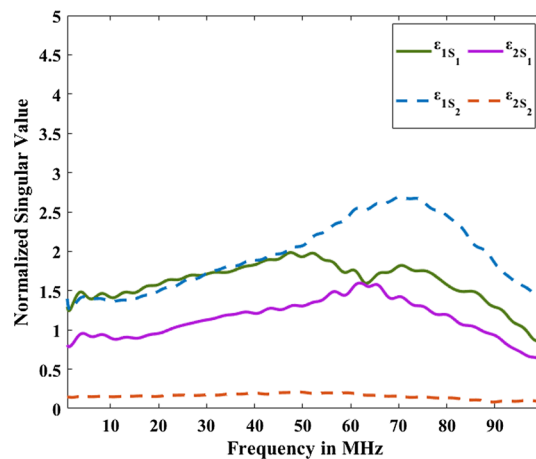
Fig. 16 Normalized downlink singular values for SDM,ξ1S1 and ξ2S1 for Scenario 1: spatially separated RX (solid lines) d1 = 100 cm, d2 = 70 cm, d3 = 70 cm, Scenario 2: (dashed lines) and ξ1S2 and ξ2S2 for Scenario 2: co-located RX:d1 = 50 cm, d2 = 5 cm, d3 = 35 cm

Table 2 Throughput evaluation of D-MIMO set-up in two different scenarios

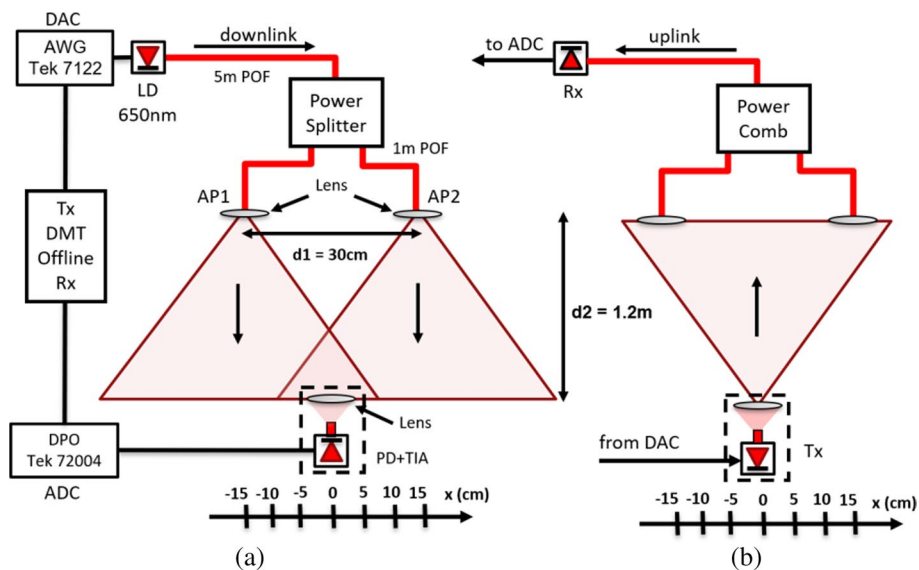| D-MIMO SDM		D-MIMO WDM	
Scenario 1	586 Mbps	Scenario 1	484 Mbps
Scenario 2	421 Mbps	Scenario 2	369 Mbps

Fig. 17 Passive DUs: schematic, where the red path refers to **a** optical downlink, **b** uplink

8.2 Results for passive all-optical OFE

To simplify the ceiling infrastructure for D-MIMO, it is attractive to avoid the need for electrical powering in the DUs (i.e. of the OFEs of the AP). One solution is to remotely feed optical fibres by a broadband LD and directly emit these signals from the fibre end, without any optical–electrical–optical conversion [32]. In Fig. 17a, b the system diagram

for the downlink and uplink is presented, respectively. The transmitter is composed of a 1×2 power splitter and one distributed feedback (DFB) LD. The LD used emits red light at 658 nm, and is directly modulated in its linear region and then butt-coupled into the POF. The red LD emits an optical power of $+2$ dBm and it is biased at 80 mA. The light beam is transmitted through 5 m of POF, split and then transmitted through 1 m POF. In the DU where APs are placed, a lens is put in front of the POF end to reduce the beam divergence. The standard polymethyl methacrylate (PMMA) POF has a numerical aperture of NA$=0.5$; thus, if no lens is used, the light exiting the POF would be launched over an angular range of $-30°$–$30°$. To create a wireless cell of 45 cm, as shown in Fig. 18, a lens is placed in a defocused position in the POF-end face. On the receiver side, the beam is received by another lens, coupled into a piece of POF and detected by an optical receiver composed of a silicon photodiode (PD) and a transimpedance amplifier (TIA). The PD$+$TIA has a detection bandwidth of 1.2 GHz.

The system schematic is presented in Fig. 17, and the implementation in the laboratory is presented in Fig. 18. The horizontal distance d_1 between the two POF ends is set to 30 cm, while the vertical distance d2 between the POF outlets and receiver is set to 1.2 m. Measurements were performed by moving the receiver along the x-axis, to simulate motion across cells. The x-axis position 0 represents the middle between both POFs-end transmitters and the positions $+15$ and -15, represent the position in front of AP1 and AP2, respectively.

To evaluate the achievable link performance considering user movement, transmissions using discrete multitone (DMT) modulation were realized. DMT, which is a (real-valued) baseband variant of OFDM, were used both for downlink and uplink. DMT was optimized by adaptive bit and power loading over 128 subcarriers, clipped at 9 dB, thus at $2\sqrt{2}$ times the rms signal strength. A bit error rate (BER) below the FEC level 1E-3 is achieved for all the presented results. An arbitrary waveform generator (AWG) works as a digital-to-analogue converter (DAC) and generates the DMT signal. At the receiver, the signal is captured by a digital phosphor oscilloscope (DPO) that works as an analogue-to-digital converter (ADC) sampling at 50 GSa/s. Offline signal processing is performed to obtain the throughput, SNR and BER counting for different positions of the user with respect to the POF outputs.

Figure 19a presents the throughput for various receiver positions for the downlink and uplink, respectively. The maximum throughput is obtained at the centre, position 0,
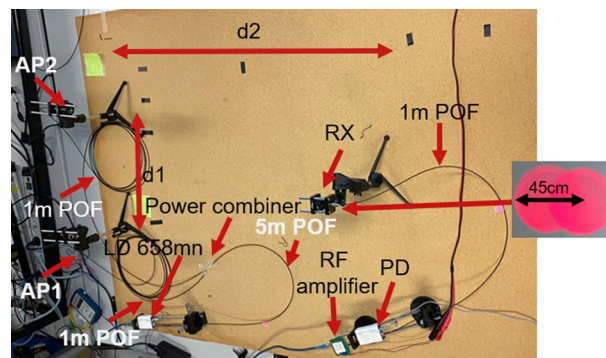

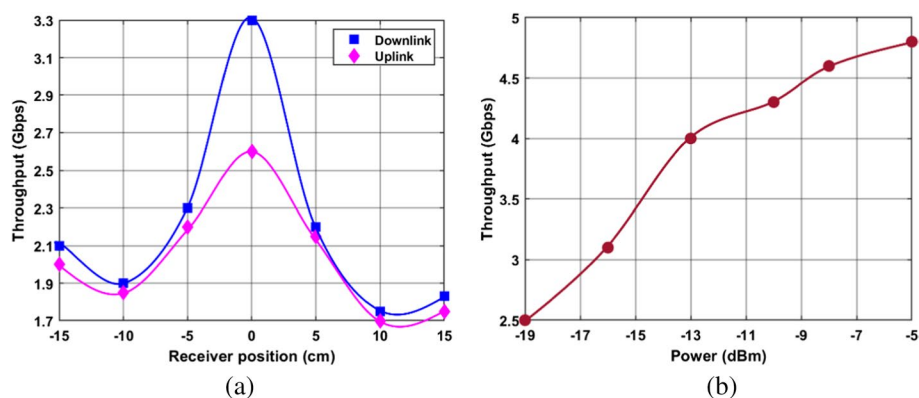**Fig. 18** Experimental set-up with passive DUs

Fig. 19 Link performance of DMT incl. 1.2 m VLC transmission for the downlink and uplink (**a**) and POF throughput without wireless for various optical power (**b**)

where the receiver is positioned in the middle of the overlapping area, achieving around 3.3 Gbps (downlink) and 2.6 Gbps (uplink) using DMT. At position 0, the receiver obtains signal contributions from both transmitters, which increases its SNR and, consequently, the throughput. When a user moves among cells, a throughput variation of 1.3–1.4 Gbps was measured. Figure 19b presents the performance of the POF output, measured directly at AP. Including wireless at $x=0$, the received power is -13.5 dBm. Using Fig. 19b for -13.5 dBm we can see a difference of 0.7 Gbps, and for $x=-10$, where the received power is -16.5 dBm, the difference becomes 1.2 Gbps. So, the user position with respect to APs has a considerable impact on the link performance.

9　MIMO performance with G.vlc and G.hn profiles

The LiFi G.9991 standard [15] adopts many technical features which are important for high-speed data transmission such as bit loading, channel estimation from a previous standard (G.9960 to G.9964) also known as G.hn and includes some LiFi-specific features like handover. As these features were already defined in G.hn, these are present in G.hn chipsets. Chipsets and development kits with (sometimes minor) circuit deviations for each wired medium are readily available [21]. This accelerates LiFi developments and market introduction. Secondly, G.hn offers a robust and stable backbone for LiFi, with gigabit connections over any wire including powerline cables, coaxial cables, copper phonelines and POF. The powerline and phoneline profiles are able to run MIMO over a 100 MHz bandwidth and SISO over a 200 MHz bandwidth. The coax profile runs only in SISO mode up to 200 MHz bandwidth. Its PHY achieves a theoretical throughput of 2 Gbps over phoneline and coax, and of 1.5 Gbps over power lines. OFDM modulation uses a bandwidth of 50, 100 or 200 MHz with a maximum of 512 subcarriers. Each subcarrier carries quadrature amplitude modulation (QAM) levels with up to 12 bits per symbol, according to an adaptive bit loading scheme. In contrast to radio standards designed for carrier-based transmission, G.hn works well over wired baseband channels and thus is well suited for LiFi channels. However, LEDs and large photodiodes are low-pass and may exhibit distortion due to nonlinearity of the LED modules; additionally, LiFi applications, as any other wireless application, can have mobile users leading

to time-varying channels. This poses the question whether G.vlc as it stands and as a derived technology from G.hn now solves all major LiFi problems.

9.1 Review of ITU-based LiFi technology in the market

The availability of chipsets [21] allowed the commercial release of practical LiFi systems and built confidence in the standard. For example, we can mention Signify's 2018 products offered a PHY rate up to 350 Mbps for downlink and 250 Mbps for uplink [33]. Meanwhile higher bit rates have also been tested. Also, Fraunhofer HHI developed an advanced combiner prototype, based on POF which is more robust against electromagnetic interference in industrial scenarios also considered in ELIoT. OFEs generally comprise a LED driver (modulator), an IR-LED for the downlink transmitter and a photodiode with transimpedance amplifier for the uplink receiver. Fraunhofer HHI manufactures OFE prototypes with higher power and improved receiver sensitivity intended for larger coverage areas in industrial scenarios. Fraunhofer HHI released a USB LiFi prototype (LiFi NEON) to reach 1 Gbit/s in the downlink [34]. This is intended for dense user scenarios, e.g. in conference and classrooms. Moreover, there is an advanced outdoor LiFi prototype manufactured which allows 1 Gbit/s over 100 m for fixed wireless access scenarios investigated in ELIoT. These various products and prototypes show that early LiFi technology is flexible enough to cover a great variety of different use cases. Office use cases demand a moderate, but guaranteed throughput in a wide coverage area. According to feedback from the professional market, fairly uniform coverage with several meters range is considered more important than world record throughput results in a tiny spot. Reliable, guaranteed low-latency QoS at some 100 Mbit/s/device satisfies the expected user experience. Gigabit performance is of interest in dense scenarios when aggregating the traffic of multiple users inside the coverage area. Up to 16 terminals can be served by the Signify LiFi AP in a managed TDMA scheme, within the coverage zone of six OFEs. OFDM allows reliable detection of signals from multiple OFEs. While the downlink uses 850 nm IR wavelength, the uplink uses 940 nm which allows full duplex communication in the future. The optical power emitted in up- and downlink is well below the eye safety limit by a 40% margin. The Signify modem combines the signals and sends the waveforms via analogue wiring to up to six ceiling-mounted OFEs. The diversity gain of the channel highly depends on the layout and the distances between all transmitters and orientation of receivers. Path loss can change quickly when the user moves around the room or rotates its device.

Meanwhile, other vendors, e.g. OLEDCOMM, offer G.9991 LiFi solutions. In the ELIoT project, various experiments were conducted to verify the performance of G.9991 in different environments both for phoneline and powerline topologies. The results of these experiments are shared in this section.

9.2 Measured performance under static conditions

The experimental set-up consists of a 2×2 MIMO LiFi system as shown in Fig. 20: On the one side of the system, there is a ceiling node representing a LiFi access point and on the other side a user node. Both user and ceiling nodes have a Maxlinear G.hn MIMO evaluation kit connected to two Trulifi optical frontends from Signify [35]. Each Trulifi transceiver has one IR-LED and one PD for bidirectional optical/electrical and
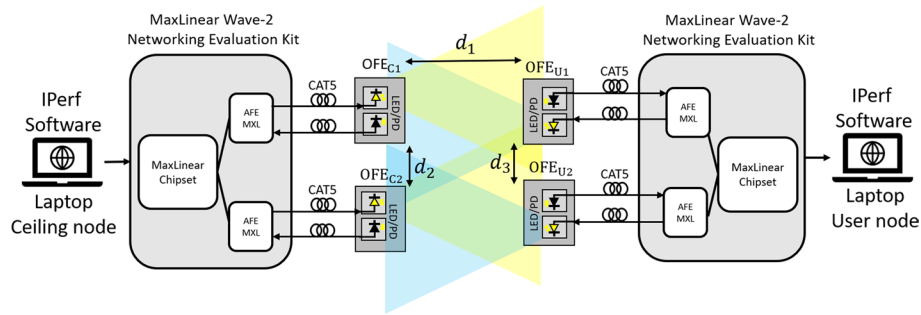
Fig. 20 Test set-up for G.vlc MIMO LiFi with phoneline or powerline profiles

electrical/optical conversion. The transceivers are connected to the evaluation kit PCBs with CAT5 cables. Connected to each evaluation kit PCB, there is one laptop running iPerf software to measure the network throughput while operating under G.hn MIMO profile.

9.3 G.hn Coax Mode: SISO with Multiple Emitters (rank K = 1)

In Coax mode, no MIMO features are available. That does not preclude the creation of diversity channel, even if we only use one photodiode in the AP ($N_R = 1$). This mimics MISO, but without the ability to apply for a transmitter phase compensation. Having calibrated our SISO model in [22], we now rely on such model: using L OFEs in the ceiling, having a pathloss h_{l1}, for the lth OFE TX to the common 1st receiver, the rate expression (1) for a distortion-free LED reduces to

$$R = \Delta_B \left\lfloor \sum_{n=1}^{N} \log_2 \left(1 + \frac{P_T}{N_T \eta_H \Gamma N_0} \left[\sum_{l=1}^{L} h_{l1} \exp \left\{ -2\pi j \frac{d_l}{c} f_n \right\} \right]^2 \right) \right\rfloor \tag{2}$$

Here, we modelled unequal cable lengths d_l causing an extra latency, dependent on the propagation speed c in the cable or POF. In fact, MIMO channel estimation could facilitate a frequency-dependent phase correction for d_l, but the Coax mode does not support that. The use of an integer (or even) number of bits per QAM constellation is reflected in the rounding brackets ⌊⌋.

Figure 21 shows a frequency response for one OFE-OFE link measured with a spectrum analyser for a typical OFE implementation, extended to a two-ray path originating from the sample signal travelling via two parallel cables. The TIA and detector produce non-white noise as also plotted in Fig. 21a. Theoretical throughputs are somewhat larger than measured throughput, firstly because of different Signal Power to Noise ratios and secondly because we have neglected distortion here. We conclude that the adaptive bit loading can track the channel and its combined interference pattern. Small differences in cabling reduce the throughput significantly, from 221 Mbit/s for equal cable lengths to 131 Mbit/s for a 3-m difference which creates one notch around 33 MHz. At very long distances, the channel response exhibits many notches and the throughput converges to 148 Mbit/s, surprisingly a bit higher than for smaller cable length differences. This throughput at unequal feeder lengths is still better than what would be achieved without
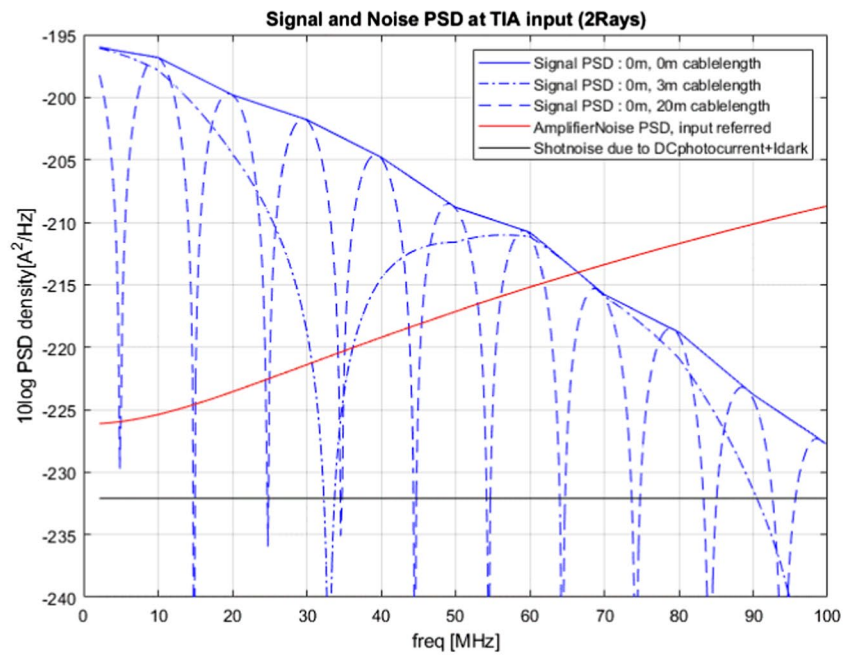
(a)
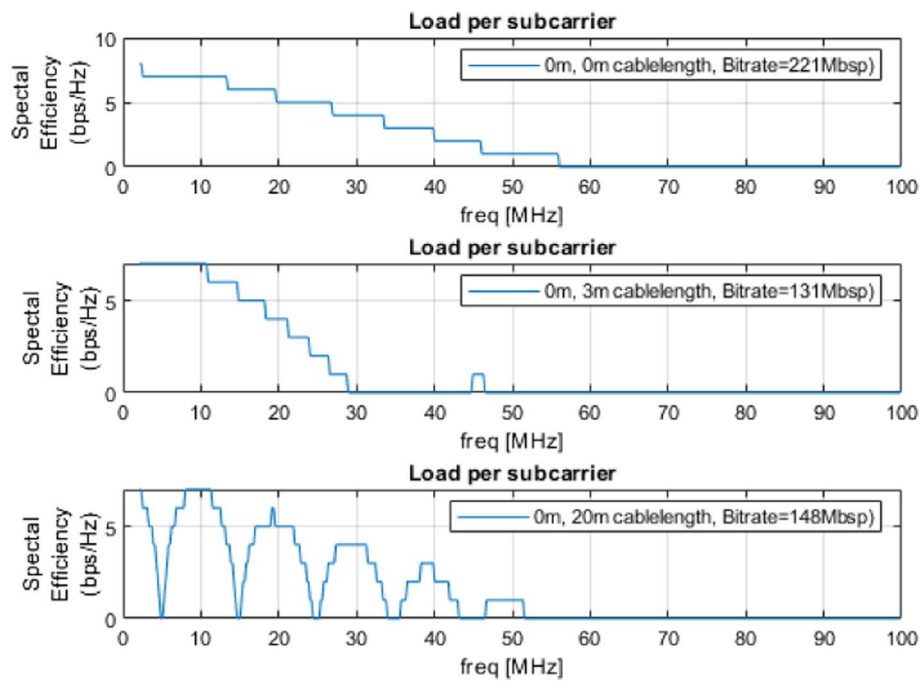
(b)

Fig. 21 **a** Received signal strength and noise floor for a two-ray SISO transmission in the middle of two emitters connected with a cable length difference of 0, 3 and 20 m. **b** Resulting estimated bit loading

adaptive bit loading, just by error correction coding across the notches. The latter coding solution is for instance used in single-frequency networks for digital audio broadcasting (DAB) where user-specific bit loading is not possible. Our bit loading is plotted in Fig. 21b.

9.4 G.hn Phoneline mode

In the first experiment, we investigate the performance of a 2×2 MIMO LiFi system using G.hn MIMO 100 MHz phoneline profile. Four different scenarios are considered and the measured throughput for each of them is shown in Table 3: In Scenario 1, the OFEs are 1 m apart from each other, i.e. $d_1 = d_2 = d_3 = 1$m. In this case, the cross talk channels have low gain, and spatial multiplexing performs well. The system achieves ~ 500 Mbps for both downlink and uplink. In the second scenario, we placed the luminaires at the user side very close to each other, i.e. $d_3 \sim 2$cm, just separated by a small angle. The user node was then placed in the middle of the coverage area of the ceiling node OFEs at a distance of 1 m. Now, the channel matrix becomes close to singular and the downlink throughput drops by more than one half and the uplink throughput decreased even more. We conclude that the system does not adapt well to handle cross talk and does not switch to a diversity mode in a highly correlated channel. In the third scenario, we kept the OFEs of the user side as in Scenario 2 but, we placed the user in front of OFE_{C2}. In this case, cross talk is very high, so a change from MIMO spatial multiplexing to spatial diversity would be required. Unfortunately, the current version of the chipset, anticipating a fixed phoneline, was not programmed to switch its transmission mode. Lacking such adaptation, the measured performance was very low. In the fourth scenario, a piece of cardboard is placed in front of OFE_{U1} to mimic a link blockage. Although one of the MIMO links is unblocked and still available for communication, the phoneline profile did not adapt well and the throughput fully collapsed.

9.5 G.hn powerline profile

In the second experiment, we used the G.hn MIMO 100 MHz powerline profile and the measured throughputs are presented in Table 4. In Scenario 5, we have again a low correlated MIMO LiFi channel, i.e. $d_1 = d_2 = d_3 = 1m$. In this case, spatial multiplexing performs well, but the achieved throughput is almost half of the achieved throughput with the phoneline profile for a similar setting. This is due to the additional overhead for more robust coding and to address PLC EMI for instance with spectral notches in the powerline profile. In Scenario 6, ceiling OFE_{C1} and user OFE_{U1} are blocked to obtain single-input single-output (SISO) performance for comparison purposes. In contrast to the performance of phoneline profile in Scenario 4, the powerline mode is able to establish communication over the unblocked link and achieve a throughput of 108 Mbps in the downlink channel, which is approximately half of the performance in Scenario 5. In Scenario 7, the OFEs at the user side are placed close to each other and placed in the middle of the coverage area—similar to Scenario 2. Although this represents a highly correlated

Table 3 Measured throughput of G.hn MIMO 100 MHz with phoneline profile

Scenario	Description	Downlink [Mb/s]	Uplink [Mb/s]
1	User-side OFEs kept 1 m apart	511	501
2	User-side OFEs put close together and placed in the middle of the coverage area	200	59.9
3	Same as [2] but user OFEs placed right below ceiling OFE_{C2}	18.5	42.3
4	Same as [1] but user OFE_{U1} blocked	0.91	3.14

channel, the measured throughput of 115 Mbps for the downlink and 112 Mbps for the uplink are much better than the phoneline case. In Scenario 8, the user node is placed in front of OFE_{C2}, and a piece of cardboard was placed in front of OFE_{C1}. The measured throughput was 108 Mb/s for the downlink and 101 Mbps for the uplink. In Scenario 9, OFE_{C1} was unblocked, and the measured throughput increases to 131 Mbps in the downlink channel and 133 Mbps in the uplink channel. For both up- and downlink directions, the MIMO options show 12% – 30% more throughput than the multiple-input single-output (MISO) arrangements where one line of sight is blocked.

9.6 Measured performance under dynamic conditions

Tests showed that some blockage is addressed as the system adapts from MIMO to MISO mode of operation. However, we also recorded instances in which the throughput collapsed after blockage and did not recover for minutes. The latter demonstrates the need for further improvement in the chipset (hardware/firmware) and the signalling to track changes in channel characteristics rapidly enough.

Figure 22 reports an experiment with Scenario 7, achieving 138 Mb/s. At 104 s, the user-side OFEs were placed in front of OFE$_{C2}$ (highly correlated channels) and the throughput reduced to 133 Mb/s. Thereafter, OFE_{C1} was blocked at 205 s, further reducing the throughput to 102 Mb/s. When the blockage was removed at around 287 s, the throughput recovered to 130 Mb/s. At 407 s, OFE$_{C2}$ was blocked which resulted in the collapse of communication for the following 60 s after which the throughput started to toggle between 20 and 50 Mb/s. When the blockage was removed at 611 s, the 130 Mb/s throughput was regained.

In summary, although the phoneline profile gives higher throughputs under static well-conditioned spatial multiplexing modes, current implementations do not cope well with channel changes. The powerline profile, despite its lower overall throughput, can handle some dynamism in the communication channel. However, since the PLC modem is developed/optimized for a powerline medium, it lacks features to handle fast changes in channel characteristics arising from mobile users in LiFi. Evidently, a new optimized mode for lighting communication is desirable. LiFi systems based on the coax profile of G.HN modems run either in SISO or MISO modes and do not exhibit the robustness against partial line-of-site blockage that 2×2 MIMO profiles have.

In ELIoT, we concluded that preferably a future generation reuses coax mode PHY parameters but extends these to MIMO. Regrettably, for obvious reasons, current IC

Table 4 Measured throughput of G.hn MIMO 100 MHz for powerline profile

| Scenario	Description	Downlink [Mb/s]	Uplink [Mb/s]
5	User-side OFEs kept 1 m apart	191	Not measured
6	Same as [5] but ceiling OFE_{C1} and user OFE_{U1} blocked	108	Not measured
7	User-side OFEs put close together and placed in the middle of the coverage area	115	112
8	Same as [7] but user OFEs placed right below ceiling OFE_{C2} and ceiling OFE_{C1} blocked	108	101
9	Same as [8] but ceiling OFE_{C1} is unblocked	131	133
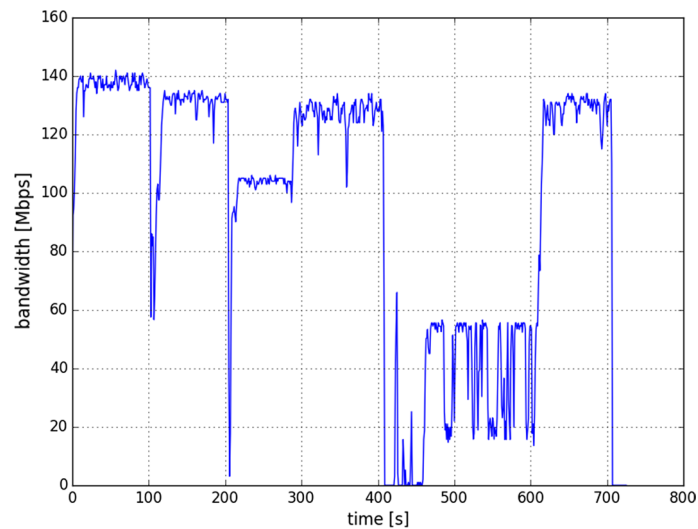
Fig. 22 Link performance when moving user-side OFEs, blocking and unblocking one of the ceiling-side OFEs

hardware makes MIMO available only in the PLC and phoneline profile, but not in the Coax mode. However, the coax PHY settings allow a higher throughput than (the SISO modes of) other profiles, because of coax choice of constellations and error correction coding. These coax settings have been proven at Technology Readiness Level 9 (i.e. in commercial products) to work well over an optical LiFi channel. Lab experiments with waveform generators indicate that these PHY choices with higher throughput per stream also work in MIMO configurations. However, we do recommend faster channel adaptation and mode switching as the LiFi channel can vary rapidly, while a coax cable is a stationary channel.

10 Roadmap for implementation

ITU-T approved the ITU-T G.9991 Recommendation for LiFi in 2020. The DCO-OFDM variant of this recommendation is the base of most developments in the ELIoT project. The goal of this recommendation is to provide a fast-to-market LiFi system with adequate performance to cover the main industrial, enterprise and residential use cases. By reusing the OFDM engine with its adaptive bit loading, already successfully used in other recommendations (i.e. in the ITU-T G.hn family, aimed to cover in-home connectivity over coaxial, phone and power lines), the resulting ITU-T G.9991 document enables LiFi systems by reusing existing chipsets. This way, early LiFi products can benefit from high-volume, low-cost integrated solutions while providing a good adaptation to the specifics of the majority of LiFi use cases. This approach allows integrators to rapidly create an early mass market for LiFi systems with a reasonable investment.

In parallel, the ITU-T Q18/15 group within ITU-T is evolving the recommendation to cover remaining and new requirements identified during the first LiFi deployments in industry. In addition, it also develops other scenarios identified in the ELIoT project that were not covered in the first version of the recommendation. Inter-domain handover and interference management is one example that has been added to the G.9991 framework

through an amendment to the standard. The work continues to add new features to the standard that will lead in the future to new amendments or a new revision of the recommendation. This will allow a new generation of LiFi chipsets that will incorporate specific LiFi hardware macros allowing new applications (e.g. positioning). New evolutions are also expected to address power reduction and better integration with other technologies to foster the adoption of LiFi technology in mobile devices. In this sense, new features have been identified within ELIoT project. Some of them can be incorporated into the current standard and in current generation chipsets through software development while others will necessitate a change of hardware and will take some time to be available since LiFi must first generate a market that is wide enough to justify a new silicon investment or to continue the strategy of piggybacking on existing implementations. Among the new required features identified by ELIoT project, we may mention faster channel estimations for enhanced mobility support, profile selection to adapt the characteristics of the transmission to the channel specifics and, last but not least, the inclusion of MIMO technologies, currently not in the standard and with limited support in the existing hardware. An evolution of MIMO techniques for LiFi as the ones investigated in the project (multi-user environments) would represent an important step in the performances achieved by LiFi systems.

Finally, we mention an integration opportunity of LED front end functionality with the existing general purpose analogue front ends used so far, for instance for PLC, Coax or phonelines.

In summary, we can say that the approach used so far allows LiFi vendors to leverage a broad portfolio of existing ITU-T G.hn compliant chipsets in their early products and facilitate interoperability of early solutions early on, reusing existing ecosystems and lowering the barriers to deploying this new technology. This approach shall be gradually transformed into more specialized LiFi solutions as the market grows and higher volumes become possible.

11 Summary

The ELIoT project addresses LiFi features that enable the next generation of IoT applications for various indoor and outdoor use cases in the industry, office, commercial and consumer sectors. We presented a distributed MIMO wireless topology which can be supported by SDM/WDM fronthaul transport of waveforms via a plastic optical fibre. Besides these, we described security aspects and various concepts for seamless handovers between the light-based access points and also to a radio-based infrastructure such as a 5G network. We have shown that the LiFi technology has the potential to provide both precise indoor localization and high-speed data transfer. The results presented indicate that the PHY offers indoor positioning, with an average accuracy of 5 cm, what even the most modern radio-based systems cannot achieve. D-MIMO light communication enhances reliability and delivers throughputs of hundreds of megabits per second. Concepts to further increase the performance of LiFi systems have already been identified. These features are currently being tested towards use-case demonstrations. We foresee that LiFi systems can complement upcoming 6G systems by offering high QoS link in hotspots. However, research challenges remain, such as making the channel adaptation faster, reduction in power, a further cost-down of the infrastructure that provides signals to all OFEs.

Abbreviations

AP	Access point
ADC	Analogue-to-digital converter
API	Application programming interfaces
AWG	Arbitrary waveform generator
MSE	Average mean square errors
BB	Baseband
BSS	Basic service set
BER	Bit error rate
CSMA/CA	Carrier-sense multiple access—collision avoidance
CSMA	Carrier-sense multiple access
CU	Central unit
CFR	Channel frequency response
CDMA	Code division
CC	Common channel
CN	Core network
DCO-OFDM	DC-biased optical orthogonal frequency division multiplexing
DAB	Digital audio broadcasting
DAC	Digital-to-analogue converter
DC	Direct current
DMT	Discrete multitone
D-MIMO	Distributed multiple-input multiple-output
DUs	Distributed units
DIY	Do-it-yourself
EMI	Electromagnetic interference
EP	End points
ELIoT	Enhance lighting for the Internet of things
EAP-AKA	Extensible authentication protocols authorization and key agreement
ITS	Intelligent transport systems
IKE	Internet key exchange
IoT	Internet of things
LD	Laser diode
LC	LiFi controller
LoS	Line of sight
LAN	Local area network
MAC	Medium access
MU	Mobile unit
MCS	Modulation and coding scheme
FDMA	Modulation frequency division
MIMO	Multiple-input multiple-output
OFEs	Optical front ends
OFDM	Orthogonal frequency division multiplexing
OWC	Optical wireless communications
PMK	Pairwise master key
PHY	Physical layer
POF	Plastic optical fibre
PMMA	Polymethyl methacrylate
PLC	Power line communication
PSD	Power spectral density
PTP	Precision time protocol
PAM	Pulse amplitude modulation
QAM	Quadrature amplitude modulation
QoS	Quality of service
RAN	Radio access network
SNR	Signal-to-noise ratio
SVD	Singular value decomposition
SDN	Software-defined networking
SDM	Space division multiplexing
SDMA	Space division multiple access
TDMA	Time division
TIA	Transimpedance amplifier
UE	User equipment
VLC	Visible light communication
WDMA	Wavelength division
WDM	Wavelength division multiplexing

the theoretical framework. KLB, MR, VJ and MW developed a reference system architecture view. AAA measured LiFi in powerline mode. PvV modelled and analysed the SISO link in coax mode. MR, PS, MW and MM reviewed and improved the presentation and text. PP and TM conceived and described the enterprise and the 5G compatible solution, respectively. MM, DB, CK and KLB devised and described the industrial use case. CK and SK devised and described the positioning solution. MMV, MR, MW and ME verified the compatibility with IC integration and with standardization. All the authors read and approved the final manuscript.

Availability of data and materials
Data sharing is not applicable to this article.

Declarations

Competing interests
The ELIoT consortium consists of industrial partners who have a common interest in a broad adoption and commercial success of LiFi and its application via standardized and interoperable solutions, and a number of independent academic partners.

References
1. W. Jiang, B. Han, M.A. Habibi, H.D. Schotten, The road towards 6G: a comprehensive survey. IEEE Open J. Commun. Soc. **2**, 334–336 (2021)
2. S. Panwar, "Breaking the Milisecond Latency Barrier," Oct 2020. [Online]. https://spectrum.ieee.org/breaking-the-latency-barrier. [Accessed 03 Aug 2021]
3. M. Müller et al., "Leverage LiFi in Smart Manufacturing," in *2020 IEEE Globecom Workshops* , (2020)
4. J.P.M.G. Linnartz et al., "ELIoT: New Features in LiFi for Next-Generation IoT," in *2021 Joint European Conference on Networks and Communications & 6G Summit (EuCNC/6G Summit)*, (2021)
5. K.L. Bober et al., "A Flexible System Concept for LiFi in the Internet of Things," in *ICTON*, (2020)
6. T. Fath, H. Haas, Performance comparison of MIMO techniques for optical wireless communications in indoor environments. IEEE Trans. Commun. **61**(2), 733–742 (2013)
7. L. Zeng et al., High data rate multiple input multiple output (MIMO) optical wireless communications using white led lighting. IEEE J. Sel. Areas Commun. **27**(9), 1654–1662 (2009)
8. P. Wilke Berenguer et al., Optical wireless MIMO experiments in an industrial environment. IEEE J. Sel. Areas Commun. **36**(1), 185–193 (2018)
9. S.M. Kouhini et al., "Distributed MIMO Experiment Using LiFi Over Plastic Optical Fiber," in *2020 IEEE Globecom Workshops* , (2020)
10. C. van den Broek and J.P. M. G. Linnartz, "A simulation study of space and time reservation multiple access," in *6th International Symposium on Personal, Indoor and Mobile Radio Communications*, (1995)
11. K.L. Bober et al., Distributed multiuser MIMO for LiFi in industrial wireless applications. J. Lightw. Technol. **39**(11), 3420–3433 (2021)
12. A. Maeder et al., "Towards a flexible functional split for cloud-RAN networks," in *2014 European Conference on Networks and Communications (EuCNC)*, (2014)
13. T. Metin, M. Emmelmann, M. Corici, V. Jungnickel, C. Kottke and M. Müller, "Integration of Optical Wireless Communication with 5G Systems," in *2020 IEEE Globecom Workshops*, (2020)
14. T.E.B. Cunha, W.X. Fan, X. Deng, J.P.M.G. Linnartz, "A Space-frequency Power Allocation Algorithm for MIMO OWC Systems over Low-Pass Channels," in *2020 1st Optical Wireless Communication Conference*, (2020)
15. International Telecommunication Union Recommendation G.9991–202104 Amd.2, "High-speed indoor visible light communication transceiver – System architecture, physical layer and data link layer specification," (2021)
16. M. Hinrichs et al., A physical layer for low power optical wireless communications. IEEE Trans. Green Commun. Netw. **5**, 4–17 (2021)
17. J. Beysens, J.P.M.G. Linnartz, D. van Wageningen, S. Pollin, TDMA scheduling in spatially extended LiFi networks. IEEE Open J. Commun. Soc. **1**, 1524–1538 (2020)
18. S.M. Kouhini et al., LiFi positioning for industry 4.0. IEEE J. Sel Top Quant Electron **27**, 1–15 (2021)
19. T.E.B. Cunha, J.P.M.G. Linnartz and X. Deng, "Throughput of Optical WDM with Wide LED Spectra and Imperfect Color-detecting Filters," in *2020 29th Wireless and Optical Communications Conference (WOCC)*, (2020)
20. S. Mardanikorani, X. Deng, J.P.M.G. Linnartz, A. Khalid, Compensating dynamic nonlinearities in LED photon emission to enhance optical wireless communication. IEEE Trans. Veh. Technol. **70**(2), 1317–1331 (2021)
21. Maxlinear, "88LX5152, 88LX5153 Wave-2 G.hn Digital Baseband (DBB) Processor," 2020. [Online]. https://www.maxlinear.com/ds/88lx515288lx5153:pdf. [Accessed 02 September 2021]
22. J.P.M.G. Linnartz, X. Deng and P. van Voorthuisen, *Impact of Dynamic LED Non-linearity on DCO-OFDM Optical Wireless Communication,* August 2021
23. IEEE, "IEEE Standard for Local and metropolitan area networks--Port-Based Network Access Control," [Online]. https://standards.ieee.org/standard/802_1X-2010.html. [Accessed 18 August 2021]

Linnartz *et al. J Wireless Com Network*   (2022) 2022:89

Page 33 of 33

24. IETF, "Internet X.509 Public Key Infrastructure Certificate and Certificate Revocation List (CRL) Profile," [Online]. https://tools.ietf.org/html/rfc5280. [Accessed 31 July 2021]
25. IETF, "Remote Authentication Dial In User Service (RADIUS)," [Online]. https://tools.ietf.org/html/rfc2865. [Accessed 09 Aug 2021]
26. IETF, "Extensible Authentication Protocol (EAP)," [Online]. https://tools.ietf.org/html/rfc3748. [Accessed 25 Sept 2021]
27. IEEE, "IEEE Standard for Information technology--Telecommunications and information exchange between systems Local and metropolitan area networks--Specific requirements - Part 11: Wireless LAN Medium Access Control (MAC) and Physical Layer (PHY) Specifications," [Online]. https://standards.ieee.org/standard/802_11-2016.html. [Accessed 12 Oct 2021]
28. J. Linnartz, On the performance of packet-switched cellular networks for wireless data communications. Wirel. Netw. **1**, 129–138 (1995)
29. H.J. Kim and J.P. Linnartz, "Virtual cellular network: a new wireless communications architecture with multiple access ports," in *IEEE Vehicular Technology Conference (VTC)*, (1994)
30. X. Wu et al., Hybrid LiFi and WiFi networks: a survey. IEEE Commun. Surv. Tutor **23**(2), 1398–1420 (2021)
31. C.R.B. Corrêa et al., "WDM over POF for D-MIMO LiFi system," in *1st Optical Wireless Communication Conference* , (2020)
32. C.R.B. Corrêa, F.M. Huijskens, E. Tangdiongga and A.M.J. Koonen, "Luminaire-Free Gigabits per second LiFi Transmission employing WDM-over-POF," in *2020 European Conference on Optical Communications (ECOC)*, (2020)
33. A.M. Khalid et al., "Productization Experiences of G.vlc (ITU) based LiFi System for high Speed Indoor Wireless Access," in *1st Optical Wireless Communication Conference (OWCC 2020)*, (2020)
34. LiFi Neon, [Online]. https://lifi-neon.de. [Accessed 05 September 2021]
35. Signify Trulifi, [Online]. https://www.assets.signify.com/is/content/PhilipsLighting/Assets/signify/global/20200416-specsheet-trulifi-6002.pdf.. [Accessed 15 April 2021]

Publisher's Note